Extended Abstracts of the 2010 International Conference on Solid State Devices and Materials, Tokyo, 2010, pp705-706

Fully Quantum Study of Silicon Devices with Scattering Based on Wigner Monte Carlo Approach

Shunsuke Koba, Ryō Aoyagi and Hideaki Tsuchiya

Kobe University, Graduate School of Eng., Dept. of Electrical and Electronics Eng.
1-1, Rokko-dai, Nada-ku, Kobe 657-8501, Japan
Phone & Fax (common): +81-78-803-6082 E-mail: 108t224t@stu.kobe-u.ac.jp

1. Introduction

The remarkable advancement in semiconductor microfabrication technology makes the manufacturing of nanoscale devices possible, where nonequilibrium transport and quantum effects directly appear on the device characteristics. To design such ultrasmall devices at normal conditions, device simulation must reliably consider both quantum and scattering effects in carrier transport.

Particle-based Monte Carlo (MC) solution of the Boltzmann transport equation (BTE) has been used to describe carrier transport within the semi-classical approximation. However, as quantum effects become more and more important with continued downscaling, the approach fails to describe the carrier transport accurately. In this study, we have developed a fully quantum MC simulator based on the Wigner transport formalism [1-4], and its ability for studying quantum and dissipative transport in Si leading-edge devices has been presented.

2. Wigner MC Approach

In the Wigner MC approach employed in this study, the equations-of-motion during a free flight are given by [3]

$$\frac{dx_i}{dt} = v \qquad (1), \qquad \frac{dk_i}{dt} = 0 \qquad (2)$$

$$\sum_{i \in M(x,k)} \frac{dA_i}{dt} = -\frac{1}{\hbar}\int_{-\infty}^{\infty} \frac{dk'}{2\pi} V(k-k',x) f_w(k',x,t) \qquad (3)$$

where V is the nonlocal potential describing quantum effects such as tunneling. A_i is an important variable called *affinity* [1], which gives wave natures of carriers into the ensemble MC technique. The Wigner MC approach has been applied to resonant-tunneling diodes, and successfully demonstrated that scattering-induced decoherence process diminishes resonant-tunneling phenomena [2,4].

3. Quantum Simulation of Si *n-i-n* Diode

Fig. 1 shows the simulated Si *n-i-n* diode and conduction band structure. We considered intra-valley acoustic phonon, inter-valley phonons including *f*- and *g*-phonons, and impurity scatterings. Here, we emphasize that all of the simulated results are compared with those of the classic MC approach based on BTE, to clarify the influence of quantum effects. Fig. 2 shows the *I-V* characteristics computed for three channel lengths. It is found that the Wigner approach provides very close results to the Boltzmann approach for L_{ch} = 10 nm and 7.5 nm, while it gives significantly larger current for L_{ch} = 5 nm. To understand such behaviors of quantum *I-V* characteristics, we first plot the microscopic quantum features for L_{ch} = 10 nm in Fig. 3. It is found that the quantum carrier distribution (Wigner) increases in the channel due to tunneling effect as shown in Fig. 3 (b), and as a result the channel potential is elevated by its space charge effect as shown in Fig. 3 (a). Contrary to the channel electrostatics, the potential in electrodes slightly descends in the close vicinity of the channel. As clearly indicated in Fig. 3 (d), this is due to the expansion of carrier depletion region caused by nonlocal quantum repulsive force from the channel potential barrier. Furthermore, as shown in Fig. 3 (c) the averaged carrier velocity decreases in the channel as compared with the Boltzmann approach, which is due to the fact that thermally-injected electrons have smaller kinetic energy because of the formation of higher potential barrier (Fig. 3 (a)), and that tunneling electrons travel more slowly than the thermally-injected ones. It is also worth noting that the averaged velocity drastically reduces in the second half of the channel, which is possibly due to a quantum reflection appearing in ballistic transport [5]. Indeed, by comparing the Boltzmann and Wigner distribution functions as plotted in Fig. 4, an interference pattern is observed in the Wigner result, which is the signature of ballistic transport with quantum reflection. It is interesting that the significant differences between the Boltzmann and Wigner approaches observed at the microscopic level are almost reduced at the macroscopic level in terms of terminal current [5].

Next, the microscopic quantum features for the shorter L_{ch} = 5 nm are also examined as shown in Figs. 5 and 6. In this extremely scaled device, the slowdown associated with tunneling and quantum reflection is mitigated, and instead carrier acceleration occurs in the access source region as in Figs. 5 (c) and 6 (b), which is due to the electric field caused by the nonlocal carrier depletion effect. Thus, the increased carrier velocity and density in the channel produce larger current density than the Boltzmann approach for L_{ch} = 5 nm as previously shown in Fig. 2.

4. Conclusions

We have shown that the Wigner MC technique is powerful in studying quantum and dissipative transport in nanoscale devices. In addition, the Wigner MC simulation has revealed that tunneling, quantum reflection and furthermore carrier transport in source region play an important role in Si devices scaled less than 10 nm.

Acknowledgements This work was supported by the Semiconductor Technology Academic Research Center (STARC).

References [1] L. Shifren et al., IEEE TED **50** (2003) 769. [2] D.

Querlioz et al., J. Comput. Electron **5** (2006) 443. [3] D. Querlioz et al., IEEE TED **54**, (2007) 2232. [4] D. Querlioz et al., PRB **78** (2008) 165306. [5] H.-N. Nguyen et al., *Proc. IWCE-13*, Beijing, 257 (2009).

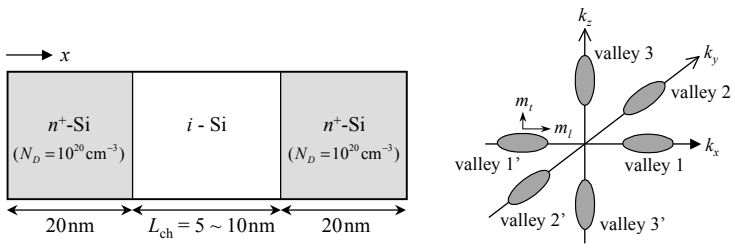

(a) (b)

Fig. 1 (a) Simulation model of Si *n*-*i*-*n* diode and (b) Si conduction band structure. The ellipsoidal multi-valleys and its band nonparabolicity are taken into account. The channel length L_{ch} is varied from 5 to 10 nm.

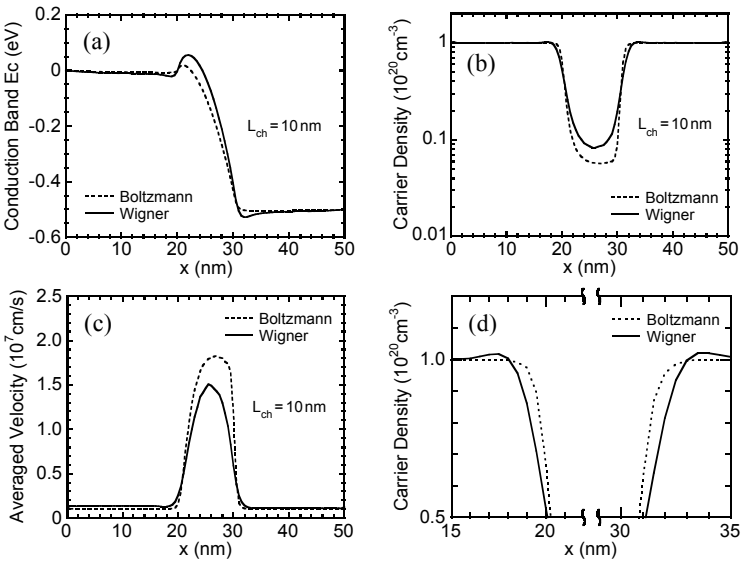

Fig. 3 (a) Potential, (b) carrier density and (c) averaged carrier velocity distributions computed at V = 0.5 V. L_{ch} = 10 nm. (d) represents the magnified carrier density distributions around the source/channel and channel/drain junctions.

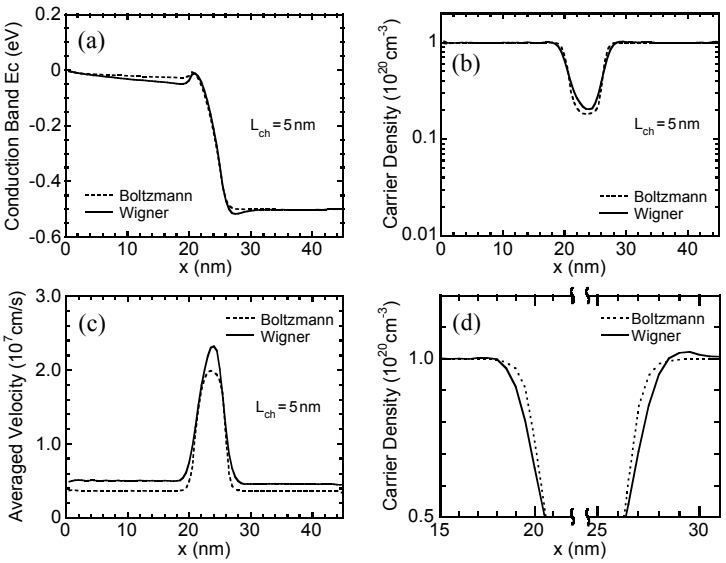

Fig. 5 (a) Potential, (b) carrier density and (c) averaged carrier velocity distributions computed at V = 0.5 V. L_{ch} = 5 nm. (d) represents the magnified carrier density distributions.

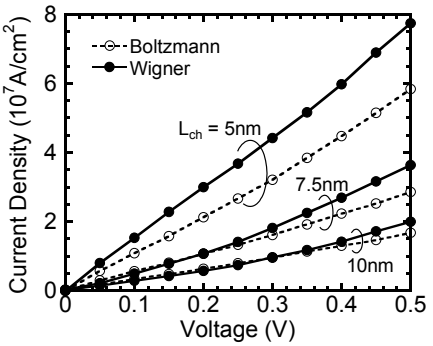

Fig. 2 *I*-*V* characteristics computed by using Boltzmann and Wigner MC methods for L_{ch} = 5, 7.5 and 10 nm.

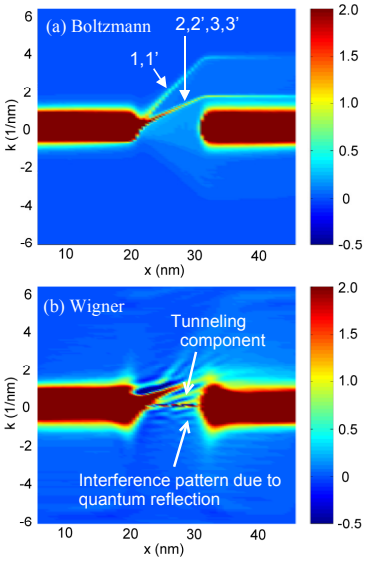

Fig. 4 Distribution functions in phase space computed by using (a) Boltzmann and (b) Wigner MC methods. V = 0.5 V and L_{ch} = 10 nm. Numbers, 1, 1', 2, 2', 3 and 3' in (a) correspond to the valley numbers in Fig. 1 (b). In (b), the distribution function is inseparable into each valley.

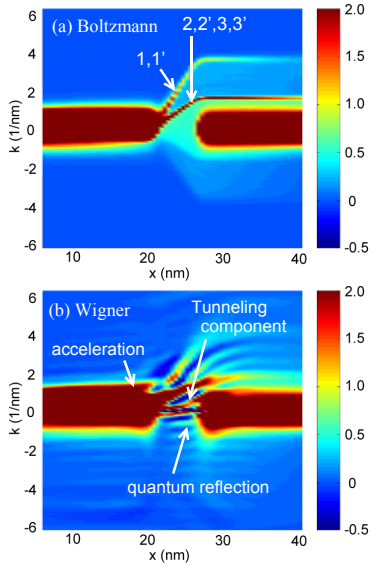

Fig. 6 Distribution functions in phase space computed by using (a) Boltzmann and (b) Wigner MC methods. V = 0.5 V and L_{ch} = 5 nm.